



HAL
open science

Robust optimization of nonlinear energy sinks used for dynamic instabilities mitigation of an uncertain friction system

Cherif Snoun, Baptiste Bergeot, Sébastien Berger

► **To cite this version:**

Cherif Snoun, Baptiste Bergeot, Sébastien Berger. Robust optimization of nonlinear energy sinks used for dynamic instabilities mitigation of an uncertain friction system. Surveillance, Vishno and AVE conferences, INSA-Lyon, Université de Lyon, Jul 2019, Lyon, France. hal-02188567

HAL Id: hal-02188567

<https://hal.science/hal-02188567>

Submitted on 18 Jul 2019

HAL is a multi-disciplinary open access archive for the deposit and dissemination of scientific research documents, whether they are published or not. The documents may come from teaching and research institutions in France or abroad, or from public or private research centers.

L'archive ouverte pluridisciplinaire **HAL**, est destinée au dépôt et à la diffusion de documents scientifiques de niveau recherche, publiés ou non, émanant des établissements d'enseignement et de recherche français ou étrangers, des laboratoires publics ou privés.

Robust optimization of nonlinear energy sinks used for dynamic instabilities mitigation of an uncertain friction system

Cherif SNOUN, Baptiste BERGEOT, Sébastien BERGER

INSA Centre Val de Loire, Université d'Orléans, Université de Tours, LaMé EA 7494,
3 Rue de la Chocolaterie, CS 23410, 41034 Blois Cedex, France

Abstract

In this paper, robust optimization tool is proposed for nonlinear energy sinks used for the mitigation of friction-induced vibrations due to mode coupling instability in braking systems. The study is based on a mechanical system which is composed of two NESs coupled to the well-known two-degrees-of-freedom Hultèn's model. In such an unstable system coupled with NES, it is usual to observe a discontinuity in the steady-state amplitude profiles which separates the parameters space into two parts which contain mitigated and unmitigated regimes respectively. We developed a methodology based on Multi-Element generalized Polynomial Chaos to identify this discontinuity which allows us to determine the Propensity of the system to undergo a Harmless Steady-State Regime (PHSSR). The objective of this work is, therefore, to maximize the value of PHSSR to obtain an optimal design of the NESs. For that, several stochastic optimization problems are presented taking into account the dispersion of the uncertain parameters.

Keywords: Brake squeal noise, Friction-induced vibrations, Nonlinear energy Sink, Uncertainties, Robust optimization

1 Introduction

Dynamic instability also named friction-induced vibrations is one of the important problem that the friction system can confront. This phenomenon can appear by the generation of Limit Cycle Oscillation (LCO) induced by dry friction. They are explained, in most studies of self-excited systems, by the coupling of the tangential and normal modes [1, 2, 3]. As a way to model these dynamic instabilities related to friction, the well-known two-degrees-of-freedom Hultèn's model [4, 5] has been widely used and it is also considered in this paper.

The NES is a nonlinear spring mass damper with a strong cubic stiffness. It can adapt itself to the main system that it is attached to without being tuned to a specific frequency. Its operation is based on the concept of Targeted Energy Transfer (TET) which has become an important passive control technique for reducing or eliminating unwanted vibrations [6, 7].

In this paper, two ungrounded NESs are used in order to mitigate or eliminate mode coupling instability in the Hultèn's model. In [8], the authors classified the steady-state response regimes in two main regimes related to the dispersion of some uncertain parameters: the first are the mitigated regimes and the second are the unmitigated regimes. As usual in the context instability mitigation by means of NESs, the LCO amplitude profile presents a discontinuity between these regimes which makes the NES potentially very sensitive to uncertainty. For that, with a low computational cost, the aim is to maximize the performance of the NES (i.e. minimize the region parameter of unmitigated regimes), by optimizing its design parameters taking into account uncertain parameters.

NES has been extensively optimized in a deterministic context (see e.g. [9]), but there is very little work performing optimization of NES under uncertainties in general [10] and for mitigation of self-excited vibrations in particular [11]. In the latter, the authors have developed a methodology of optimization under uncertainties of a NES attached to a two-degree-of-freedom airfoil. In the present work, a robust optimization tool based on the Multi-Element generalized Polynomial Chaos (ME-gPC) is developed.

The article is constructed as follows: in Section 2, the two degrees-of-freedom Hultèn's model coupled to two NESs is presented. In Section 3, the steady-state of the system as well as the discontinued profile are introduced. The optimization formulation under uncertainties is formulated in Section 4. Section 5 describes

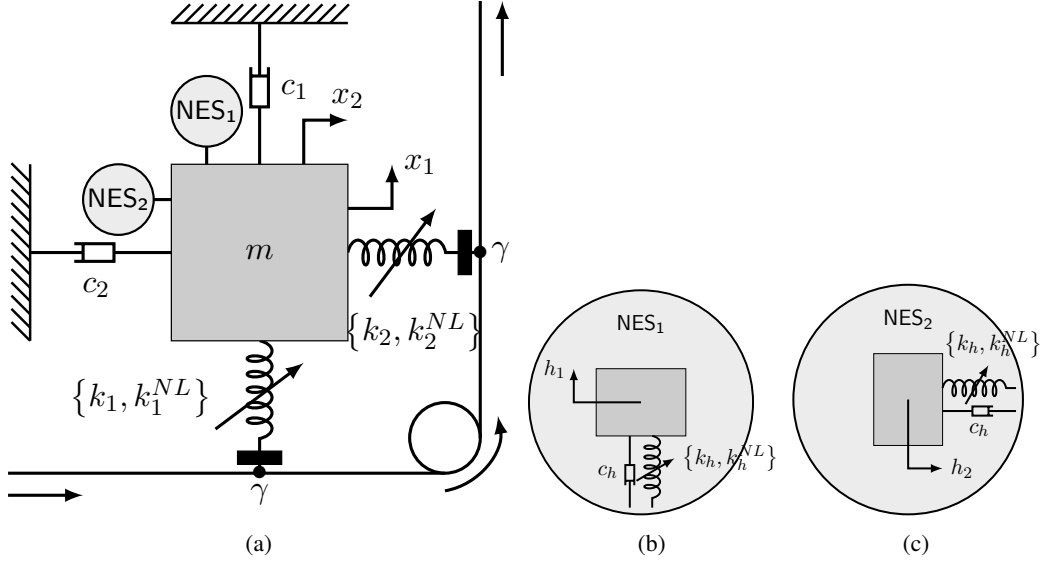


Figure 1: (a) Mechanical system with NESs. (b) Zoom on the NES₁. (c) Zoom on the NES₂.

the polynomial chaos theory and the used stochastic optimization algorithm. The results of the optimization methods are presented in Section 6. Finally, conclusions are given in Section 7.

2 The mechanical system

The mechanical system considered in this work is composed by the two degrees-of-freedom (DOF) Hult en's model [4, 5], which represents the primary system, coupled to two identical NESs with masses m_h , damping coefficients c_h and cubic stiffnesses k_h^{NL} . The NESs are attached on the primary system in an ungrounded configuration as shown in Fig. 1.

The equations which describe the mechanical system are given by :

$$\begin{aligned} \frac{d^2x_1}{dt^2} + \eta_1\omega_1\frac{dx_1}{dt} + \omega_1^2x_1 - \gamma\omega_2^2x_2 + \varphi_1x_1^3 - \gamma\varphi_2x_2^3 + \\ \mu\omega_1\left(\frac{dx_1}{dt} - \frac{dh_1}{dt}\right) + \xi_h(x_1 - h_1) + \varphi_h(x_1 - h_1)^3 = 0 \end{aligned} \quad (1a)$$

$$\varepsilon\frac{d^2h_1}{dt^2} + \mu\omega_1\left(\frac{dh_1}{dt} - \frac{dx_1}{dt}\right) + \xi_h(h_1 - x_1) + \varphi_h(h_1 - x_1)^3 = 0 \quad (1b)$$

$$\begin{aligned} \frac{d^2x_2}{dt^2} + \eta_2\omega_2\frac{dx_2}{dt} + \omega_2^2x_2 + \gamma\omega_1^2x_1 + \gamma\varphi_1x_1^3 + \varphi_2x_2^3 + \\ \mu\omega_1\left(\frac{dx_2}{dt} - \frac{dh_2}{dt}\right) + \xi_h(x_2 - h_2) + \varphi_h(x_2 - h_2)^3 = 0 \end{aligned} \quad (1c)$$

$$\varepsilon\frac{d^2h_2}{dt^2} + \mu\omega_1\left(\frac{dh_2}{dt} - \frac{dx_2}{dt}\right) + \xi_h(h_2 - x_2) + \varphi_h(h_2 - x_2)^3 = 0, \quad (1d)$$

where $h_1(t)$ and $h_2(t)$ (respectively $x_1(t)$ and $x_2(t)$) represent the NESs displacements (respectively the displacements of the primary system), $\eta_i = c_i/\sqrt{mk_i}$, $\omega_i = \sqrt{k_i/m}$, $\varphi_i = k_i^{NL}/m$ (with $i = 1, 2$), $\varepsilon = m_h/m$ assuming $0.01 < \varepsilon < 0.1$, $\xi_h = k_h/m$, $\mu = c_h/\sqrt{mk_1}$ and $\varphi_h = k_h^{NL}/m$.

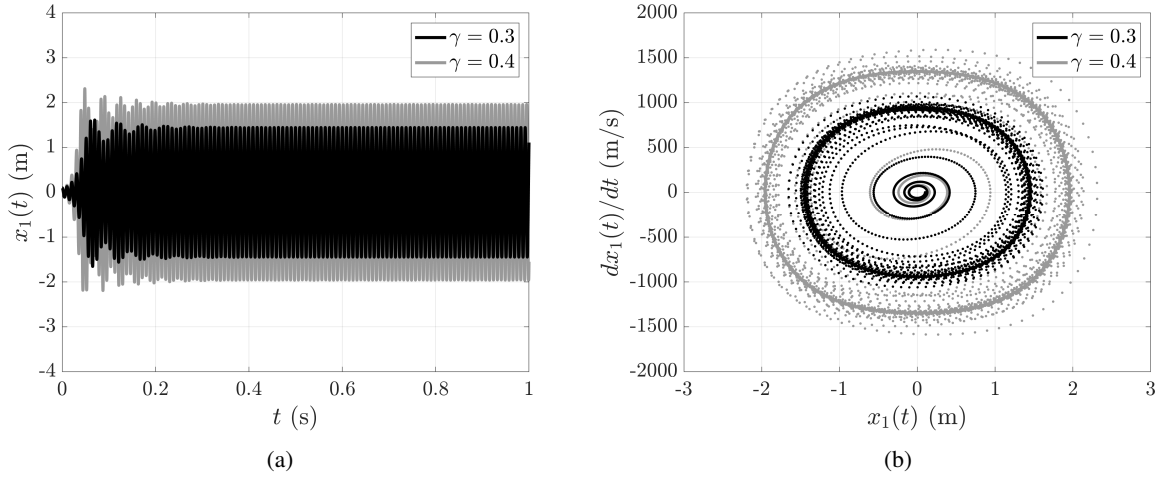


Figure 2: Numerical integration in the direction x_1 of the Hult'en's model without NESs for two values of the friction coefficient: (a) Times series; (b) Representation in the phase plane.

3 Preliminary results

3.1 Vibratory levels and possible steady-state regimes

A example of the numerical simulation of the system without NESs is plotted in Fig. 2 for two different values of the friction coefficient: $\gamma = 0.3$ and $\gamma = 0.4$. The other parameters are

$$\begin{aligned} \omega_1 &= 2\pi 100, & \omega_2 &= 2\pi 85, \\ \eta_1 &= 0.02, & \eta_2 &= 0.06, & \varphi_1 &= 10^5, & \varphi_2 &= 0, \\ \varepsilon &= 0.05, & \xi_h &= 0.001, & \mu &= 0.02, & \varphi_h &= 1.4 \cdot 10^5. \end{aligned} \quad (2)$$

Moreover, the initial conditions are small perturbation of the trivial equilibrium position: $x_1(0) = x_2(0) = 0$, $\dot{x}_1(0) = \dot{x}_2(0) = 10$. When $\gamma = 0.4$, Limit Cycle Oscillations (LCO) are observed. We focus our analysis on the capacity of the NESs to suppress or mitigate these LCOs.

Four main types of steady-state regimes can be generated when two NESs is attached on the: complete suppression of the instability, mitigation through Periodic Response (PR), mitigation through Strongly Modulated Response (SMR) or no mitigation.

An illustration of these regimes is shown in Fig. 3 which plots the displacements $x_1(t)$ with respect to times with and without the NESs. Hereafter, mitigated regimes referred to complete suppression, PR and SMR.

3.2 The objective function

We define the amplitude A_1^{wNES} of the variables x_1 of the coupled system Eq. (1) and within a steady-state regime as

$$A_1^{wNES} = \frac{\max [x_1^{SSR}(t)] - \min [x_1^{SSR}(t)]}{2}, \quad (3)$$

where $x_1^{SSR}(t)$ is the times series of the variables x_1 obtained from the numerical integration of the coupled system Eq. (1) within the steady-state regime¹.

The amplitudes A_1^{wNES} and A_1^{woNES} (i.e. the amplitude of the system without NESs) are plotted as a function of the friction coefficient γ in Fig. 4 for the set of parameters Eq. (2).

The figure highlights a jump (or discontinuity) in the amplitude profile A_1^{wNES} . This discontinuity corresponds, when γ increases, to the transition from SMR to no suppression regimes and separates mitigated regimes and unmitigated regimes. The value of γ at the jump is called mitigation limit (with respect to γ) and denoted γ_{ml} .

¹The calculation was performed on 4 seconds in order to be sure that the steady-state has been reached.

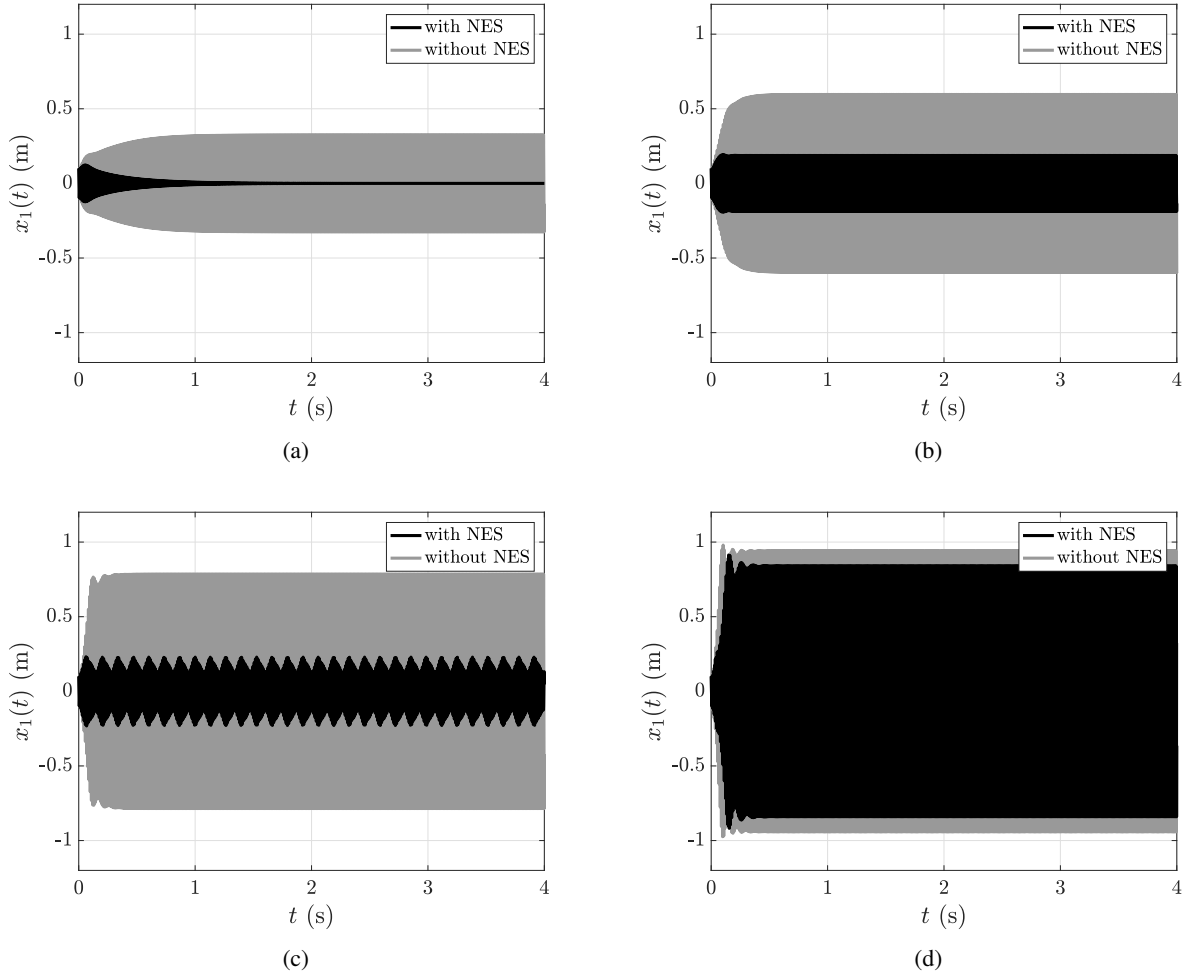


Figure 3: Comparison between time serie $x_1(t)$ resulting from the numerical integration of the braking system with and without NESs. (a) Complete suppression, $\gamma = 0.16$; (b) Mitigation: PR, $\gamma = 0.18$; (c) Mitigation: SMR, $\gamma = 0.2$; (d) No suppression, $\gamma = 0.22$. The set of parameters Eq. (2) is used.

Then the Propensity of the system to undergo a Harmless Steady-State Regime (PHSSR) of the oscillation by the NESs is estimated. We compute a set of S_{total} samples of the uncertain parameters within the considered uncertain space and following their distribution law. Then, the PHSSR is defined as follows

$$\text{PHSSR} = \frac{S_{\text{HSSR}}}{S_{\text{total}}} \times 100 \quad (4)$$

where S_{HSSR} is the number of samples within the region of uncertain parameters space in which the LCO of the system is mitigated or the system is stable.

The PHSSR represents the objective function of the study.

4 Optimization Formulation under uncertainties

The sensitivity of the friction coefficient is such that the steady state of the mechanical system is discontinuous and presents a jump. This jump induces areas in which the efficiency of the NES is either high or low. In order to obtain a robust design of NES which is insensitive to the dispersion of the uncertain parameters, a stochastic optimization problem is considered as follow:

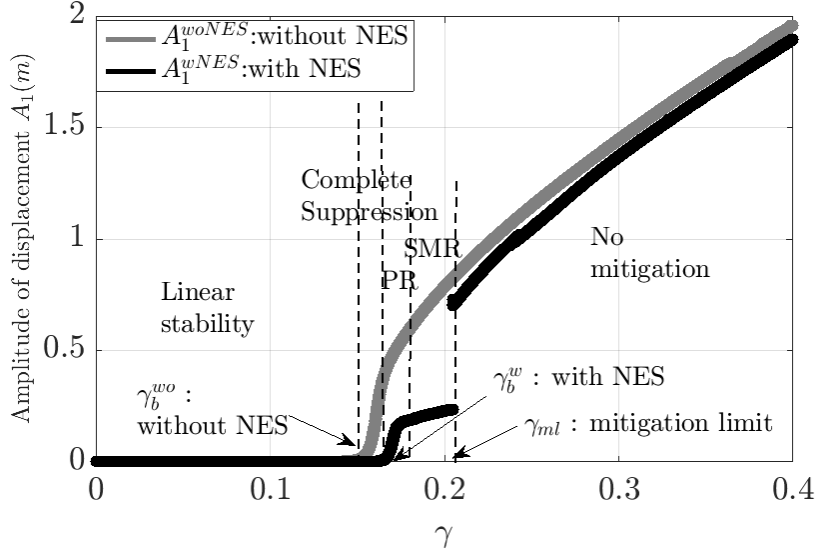


Figure 4: Amplitudes A_1^{wNES} and A_1^{woNES} as a function of the friction coefficient γ .

$$\begin{aligned}
 & \text{Maximize} && PHSSR(A_1^{wNES}(x_d, x_u)) \\
 & \text{Subject to} && x_d^{(min)} \leq x_d \leq x_d^{(max)}
 \end{aligned} \tag{5a}$$

$$\tag{5b}$$

where

- x_d represents the design variables of the NES with lower bounds $x_d^{(min)}$ and upper bounds $x_d^{(max)}$.
- x_u represent the uncertain parameters of the primary system.

5 Optimization Algorithm

In order to solve an optimization problem under uncertainties, the determination of the LCO of the mechanical system need to use a stochastic method to take into account the uncertain parameters. In this work, the Multi-Element generalized Polynomial Chaos is used as an alternative approach to reduce the computational cost of the traditional methods (Monte Carlo or deterministic simulations).

5.1 Polynomial Chaos theory

5.1.1 generalized Polynomial Chaos

The gPC theory [12, 13] allows to express a random process $X(\xi)$ called also the Quantity of Interest (QoI) with a truncated orthogonal polynomial function series such as

$$X(\xi) \approx \sum_{j=0}^{N_p} \bar{x}_j \phi_j(\xi), \tag{6}$$

where:

- \bar{x}_j are the gPC coefficients of the stochastic process $X(\xi)$,
- $\phi_j(\xi)$ are orthogonal polynomial functions,
- $N_p = \frac{(p+r)!}{p!r!} - 1$ where p is the order of the gPC and r is the number of the uncertain parameters,
- $\xi(\xi_1, \dots, \xi_r)$ is a vector of r independent random variables within $[-1, 1]^r$.

5.1.2 Multi-Element Generalized Polynomial Chaos (ME-gPC)

The ME-gPC consists to split ξ into a collection of m non-intersecting elements and to approximate the stochastic process $X(\xi)$ using the gPC in each element [14]. It is given by

$$X(\xi) \approx \sum_{k=1}^m X_k(\bar{\xi}^k) J_k, \quad (7)$$

where

- $X_k(\bar{\xi}^k) = \sum_{j=1}^{N_p} \bar{x}_{k,j} \phi_j(\bar{\xi}^k)$ where $\bar{\xi}^k$ is an uniform random variables corresponding to the k^{th} element,
- J_k is the element size.

We denote by $\sigma_{p,k}^2$ the variance of the QoI estimated in the k^{th} element directly from the gPC coefficients as:

$$\sigma_{p,k}^2 = \frac{1}{2^r} \sum_{j=1}^{N_p} \bar{x}_{k,j}^2 \langle \phi_j^2 \rangle. \quad (8)$$

5.2 Proposed algorithm

The ME-gPC metamodel would not be efficient in its initial configuration due to the presence of discontinuities. In fact, the goal is not to obtain an accurate representation of the response of the system, but to be able to locate the discontinuity. Figure 5 shows the different steps of the ME-gPC based method to detect the jump. The method consists to split the stochastic parameter space into two equal non-intersecting elements and to evaluate in each element the amplitude of displacement of the system. Then, the verification of the presence or not of discontinuity is addressed according to the comparison of the variance $\sigma_{p,k}^2$ to a chosen threshold θ_1 . The process stops either if the element size reaches a threshold

$$J_{kmin} = \theta_2 J_{k0}, \quad (9)$$

where J_{k0} represents the size of the initial element or if the number N' of numerical simulations required with the ME-gPC based method is smaller than the typical number N of simulations required with the reference method. The mitigation limit is, therefore approximated by the upper bound of the last found element and then the robust evaluation of the PHSSR is calculated.

6 Results

In this work, the friction coefficient γ is considered as the uncertain parameter (x_u) and the damping rate of the NES μ as the design variables (x_d).

6.1 Reference study

In this section, the reference is evaluated with the deterministic model (1). In the first case, 50 deterministic samples of the damping rate of the NES ($\mu \in [0, 0.04]$) are used. For each sample of μ , 1000 samples of the friction coefficient ($\gamma \in [0, 0.4]$) are used in order to determine the mitigation limit γ_{ml} . The number of simulations is therefore equal to 50000 (50×1000). Fig. 6(a) shows the variation of the mitigation limit as a function of μ . Because of the presence of a plateau, we realize that the number of samples of γ is not sufficient to determine the optimal design value of μ . For that, 10 added deterministic samples of the damping rate of the NES ($\mu \in [0.02, 0.03]$) with now 10000 samples of the friction coefficient γ to determine the mitigation limit. The total number of simulations required is now equal to 150000 ($50000 + 10 \times 10000$). Fig. 6(b) shows the new variation of the mitigation limit as a function of μ . In this case, the maximum (i.e. optimal) value of γ_{ml} is 0.2004 which gives a maximum value of PHSSR equals to 50.1%. The corresponding optimal design value for the damping rate is $\mu_{opt}^{Ref} = 0.024$.

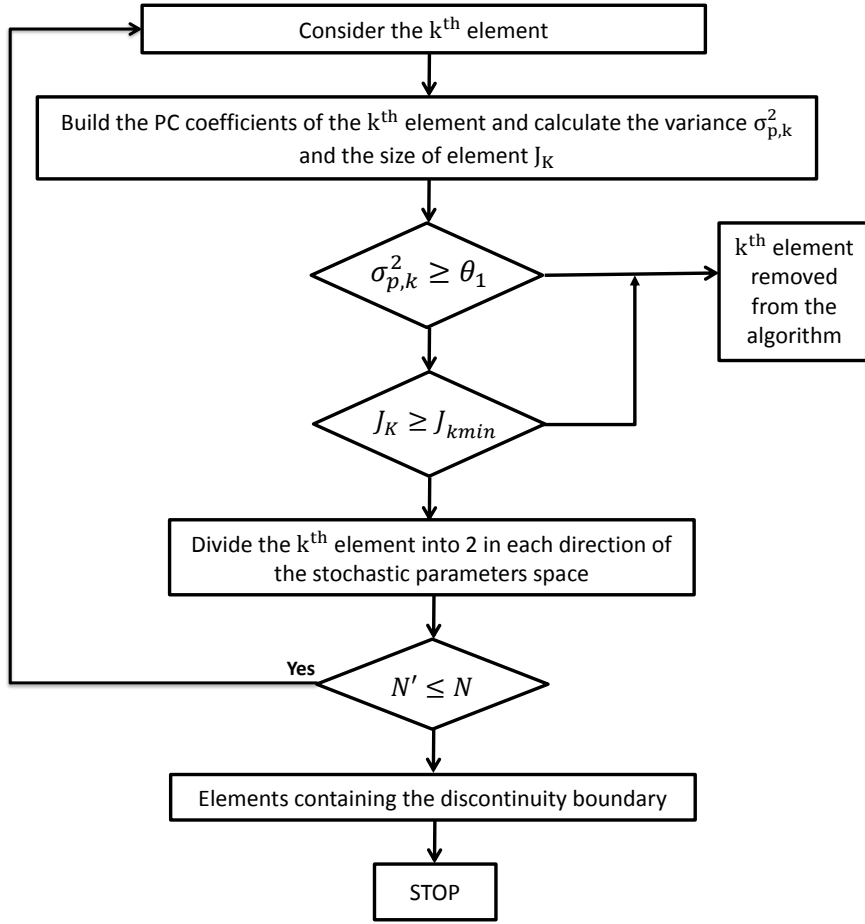


Figure 5: Algorithm of the ME-gPC based method to identify the mitigation limit.

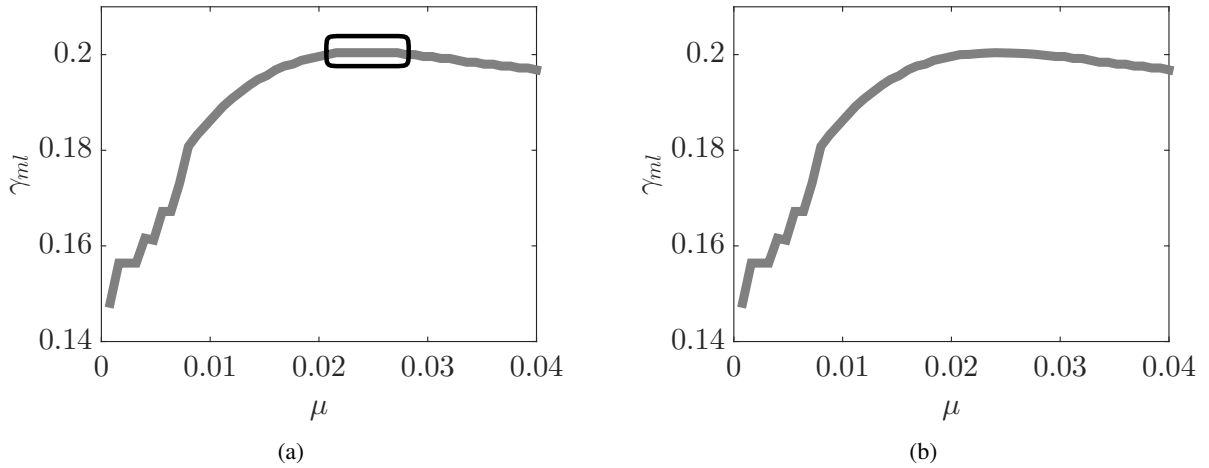


Figure 6: Variation of the mitigation limit as a function of the damping ratio of the NES (μ) by the deterministic method. (a) 50 samples of $\mu \in [0, 0.04]$; (b) 10 added samples of $\mu \in [0.02, 0.03]$.

6.2 Optimization using the ME-gPC based method

In this section, the algorithm presented in Fig. 5 is applied to estimate A_1^{wNES} (the considered QoI) and then the mitigation limit and the PHSSR. The gPC order is $p = 1$ and the threshold $\theta_1 = 2.10^{-3}\%$. Fig. 7 shows an example, with a given value of μ , of the algorithm described in Section 5.2. As described above, the mitigation limit is approximated by the upper bound of the last found element. Now, 50 deterministic samples of the damping rate of the NES ($\mu \in [0, 0.04]$) are used. The samples of the friction coefficient γ are built

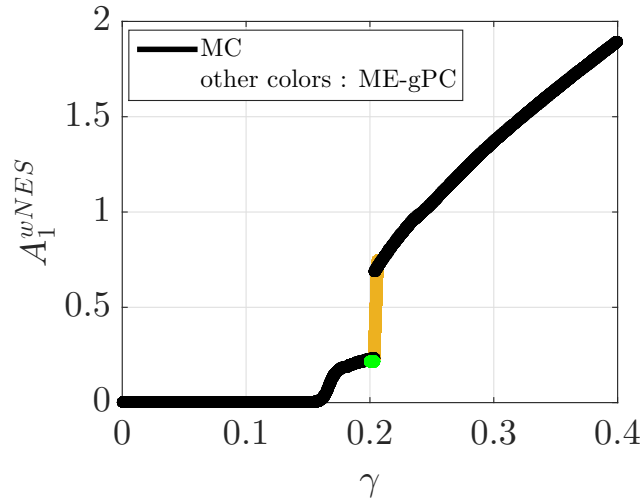


Figure 7: Last step of the ME-gPC based method to identify of the mitigation limit (γ_{ml}).

using the Latin Hypercube Samples (LHS) method. Fig. 8(a) shows the variation of the mitigation limit as a function of μ with $\theta_2 = 1\%$. In this case, the number of simulations is equal to 6547. The optimal value of μ is in the interval $I_{opt,1} = [0.016, 0.032]$. In order to reduce the size of I_{opt} the threshold θ_2 and the mitigation limit is determined within $I_{opt,1}$. Fig. 8(b) shows the variation of the mitigation limit as a function of μ with $\theta_2 = 0.1\%$. The added number of simulations is equal to 2766 and the optimal value of μ is in the interval $I_{opt,2} = [0.019, 0.026]$. Fig. 8(c) shows the variation of the mitigation limit as a function of μ with $\theta_2 = 0.05\%$ used within $I_{opt,2}$. In this case, the added number of simulations is equal to 1395 and the optimal value of μ is now in the interval $I_{opt,2} = [0.0208, 0.0248] = 0.0228 \pm 8\%$. This interval has a midpoint equal to 0.0228 which gives a relative error equal to 5% compared to the reference. The total number of simulations is equal to 10708 which represents 14 times less than the reference.

7 Conclusion

In this paper, the optimization of two NESs attached to the two degrees-of-freedom (DOF) Hultén's model is presented. It accounts the discontinuity presented in the steady-state profiles using a stochastic optimization method. The results show the efficiency of the ME-gPC based method to detect the discontinuity and therefore the so-called mitigation limit. This allows us to provide an optimal design of the NESs with a low computational cost compare to that the deterministic optimization reference method.

References

- [1] J.T. Oden and J.A.C. Martins. Models and computational methods for dynamic friction phenomena. *Computer Methods in Applied Mechanics and Engineering*, 52(1):527–634, 1985.
- [2] Guillaume Fritz, Jean-Jacques Sinou, Jean-Marc Duffal, and Louis Jézéquel. Investigation of the relationship between damping and mode-coupling patterns in case of brake squeal. *Journal of Sound and Vibration*, 307(3):591–609, 2007.
- [3] B. Hervé, J.-J. Sinou, H. Mahé, and L. Jézéquel. Analysis of squeal noise and mode coupling instabilities including damping and gyroscopic effects. *European Journal of Mechanics - A/Solids*, 27(2):141–160, mar 2008.
- [4] J. Hultén. Friction phenomena related to drum brake squeal instabilities. In *ASME Design Engineering Technical Conferences, Sacramento, CA*, 1997.

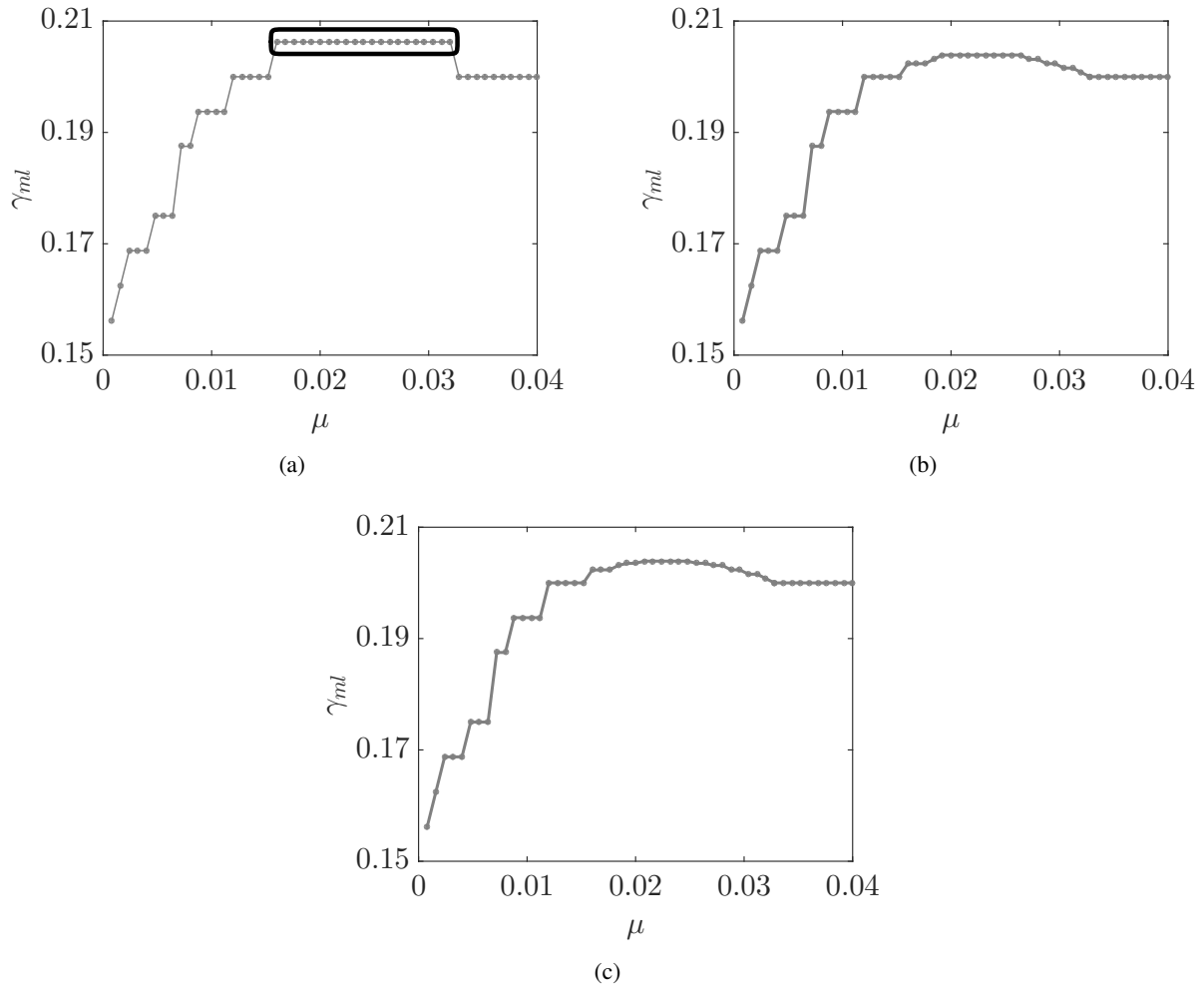


Figure 8: Variation of the mitigation limit as a function of the damping ratio of the NES using the ME-gPC based method. (a) $\theta_2 = 1\%$; (b) $\theta_2 = 0.1\%$; (c) $\theta_2 = 0.05\%$.

- [5] J. Hultén. Brake squeal - a self-exciting mechanism with constant friction. In *SAE Truck and Bus Meeting, Detroit, Mi, USA*, 1993.
- [6] A.F. Vakakis and O.V. Gendelman. Energy pumping in nonlinear mechanical oscillators: Part II - Resonance capture. *Journal of Applied Mechanics*, 68:42–48, 2001.
- [7] A. F. Vakatis, O. V. Gendelman, L. A. Bergman, D. M. McFarland, G. Kerschen, and Y. S. Lee. *Nonlinear Targeted Energy Transfer in Mechanical and Structural Systems*. Springer-Verlag, Berlin, New York, 2008.
- [8] B Bergeot, S Berger, and S Bellizzi. Mode coupling instability mitigation in friction systems by means of nonlinear energy sinks : numerical highlighting and local stability analysis. *Journal of Vibration and Control*, 24(15):3487–3511, 2017.
- [9] Tuan Anh Nguyen and Stéphane Pernot. Design criteria for optimally tuned nonlinear energy sinks—part 1: transient regime. *Nonlinear Dynamics*, 69(1-2):1–19, nov 2011.
- [10] Ethan Boroson, Samy Missoum, Pierre-Olivier Mattei, and Christophe Vergez. Optimization under uncertainty of parallel nonlinear energy sinks. *Journal of Sound and Vibration*, 394:451 – 464, 2017.
- [11] Bharath Pidaparathi and Samy Missoum. Stochastic optimization of nonlinear energy sinks for the mitigation of limit cycle oscillations. *AIAA Journal*, pages 1–11, jan 2019.
- [12] Roger G. Ghanem and Pol D. Spanos. *Stochastic finite elements: A spectral approach*. 1991.

- [13] R.H. Cameron and W.T. Martin. The orthogonal development of non-linear functionals in series of fourier-hermite functionals. *Annals of Mathematics*, 48(2):385–392, 1947.
- [14] Xiaoliang Wan and George Em Karniadakis. An adaptive multi-element generalized polynomial chaos method for stochastic differential equations. *Journal of Computational Physics*, 209(2):617 – 642, 2005.